TASK 4(NORMAL)

~~POWER~~

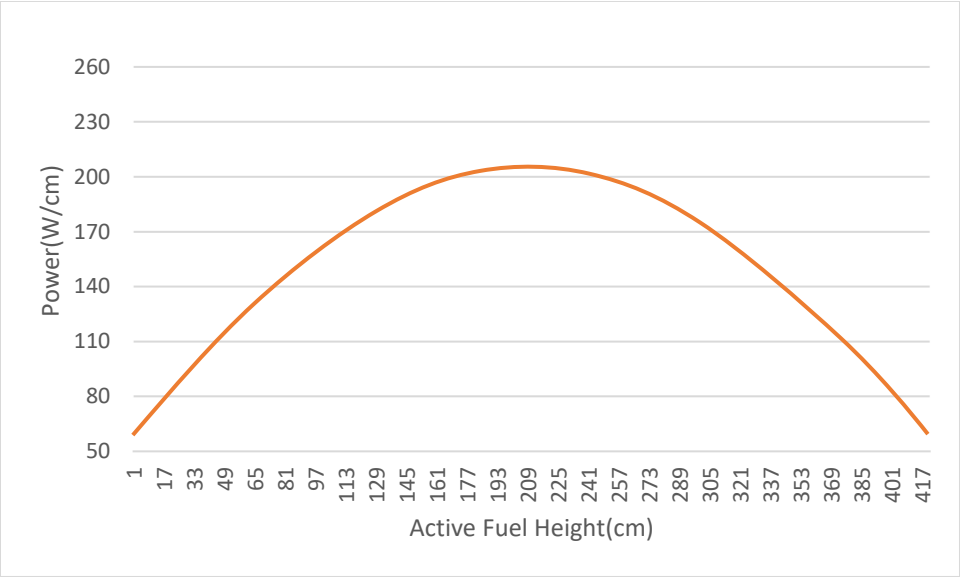

~~TEMP~~

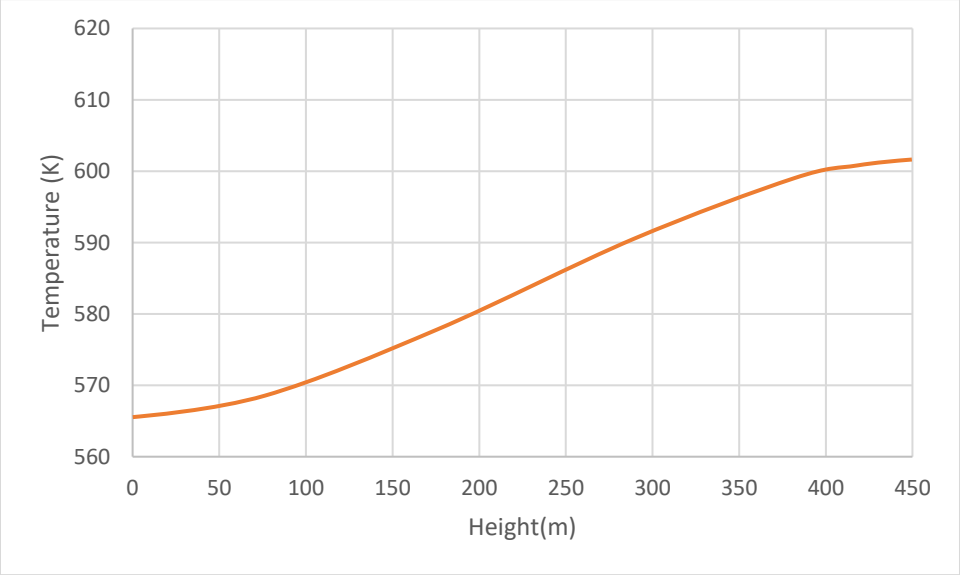

~~ENTHALPY~~

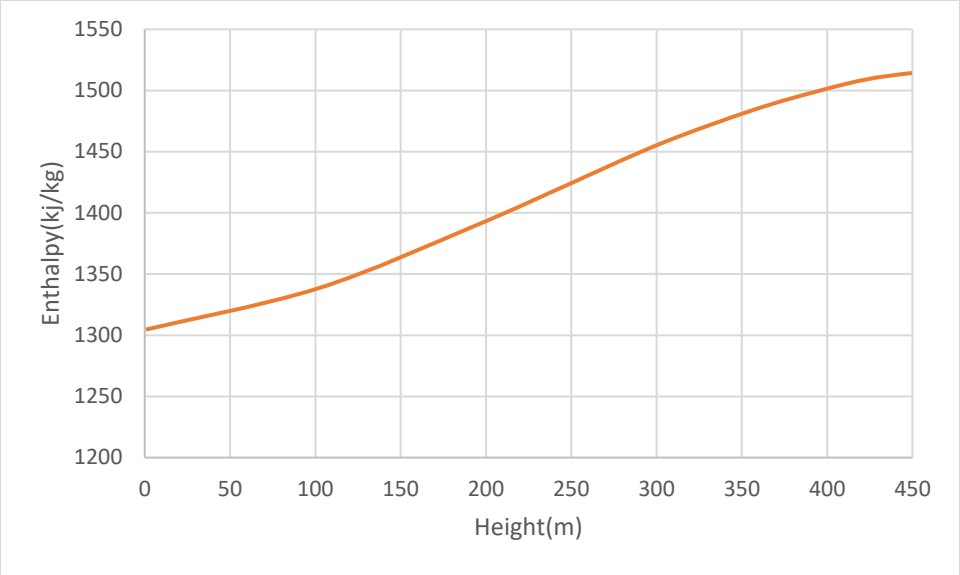

~~PRESSURE~~

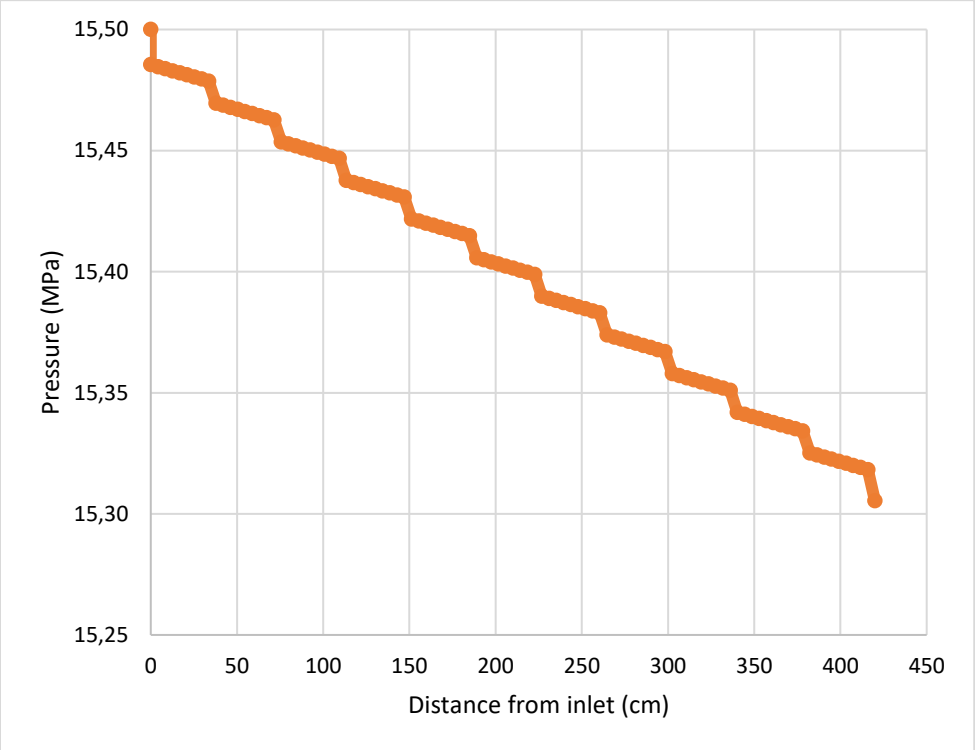

~~PRESSURE/MASSFLUX~~

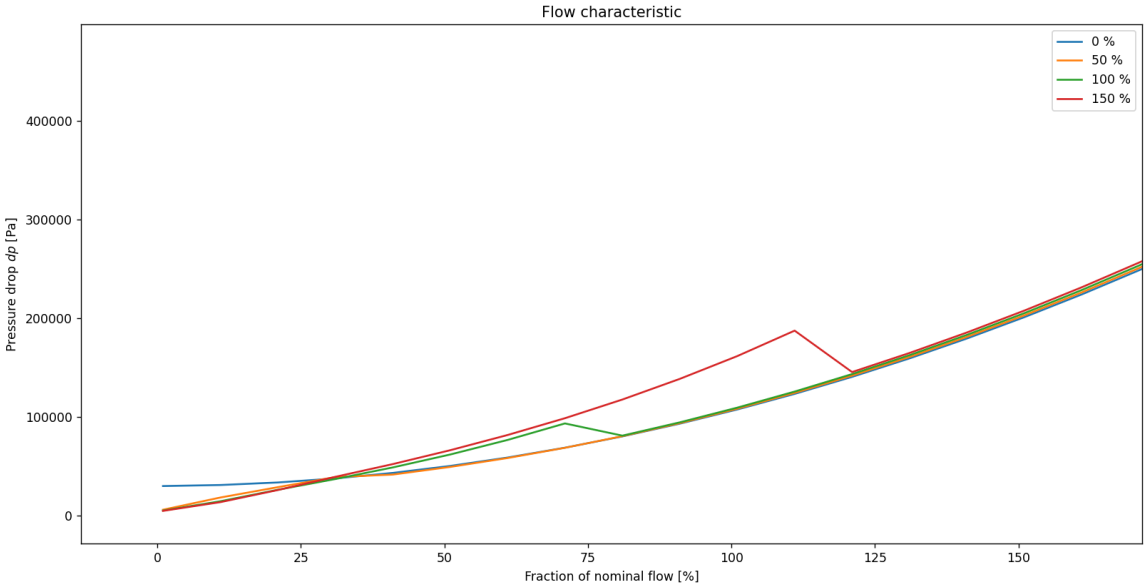

The temperature was determined to be slightly different from the literature value at 600.82K compared to 601.85K, while the inlet enthalpy was calculated to be 1.309 x 106 J/kg·K using XSteam at 294.85°C and 155 bar. The total pressure drop was comparable to the literature value, with 0.188 MPa and 0.195 MPa, respectively, indicating reliable calculations. The inlet orifice coefficient was measured to be 0.8.

The flow characteristics were analyzed at various power levels. Single-phase steam was observed at very low flow rates for 150%, 100%, and 50% power, and 2-phase flow was observed at medium flow rates. The transition from single-phase steam to 2-phase flow was indicated by an upward bump in the curve. Single-phase water was observed at high flow rates, and the transition from 2-phase flow to single-phase water was marked by a downward bump. At 0% power, there was only continuous single-phase water due to the absence of heat energy. Interestingly, the total pressure was higher for 0% power at very low flow rates because of the presence of single-phase water instead of single-phase steam, leading to higher gravity and friction pressure drops.

TASK5(HOT CAHNNEL)

~~POWER~~

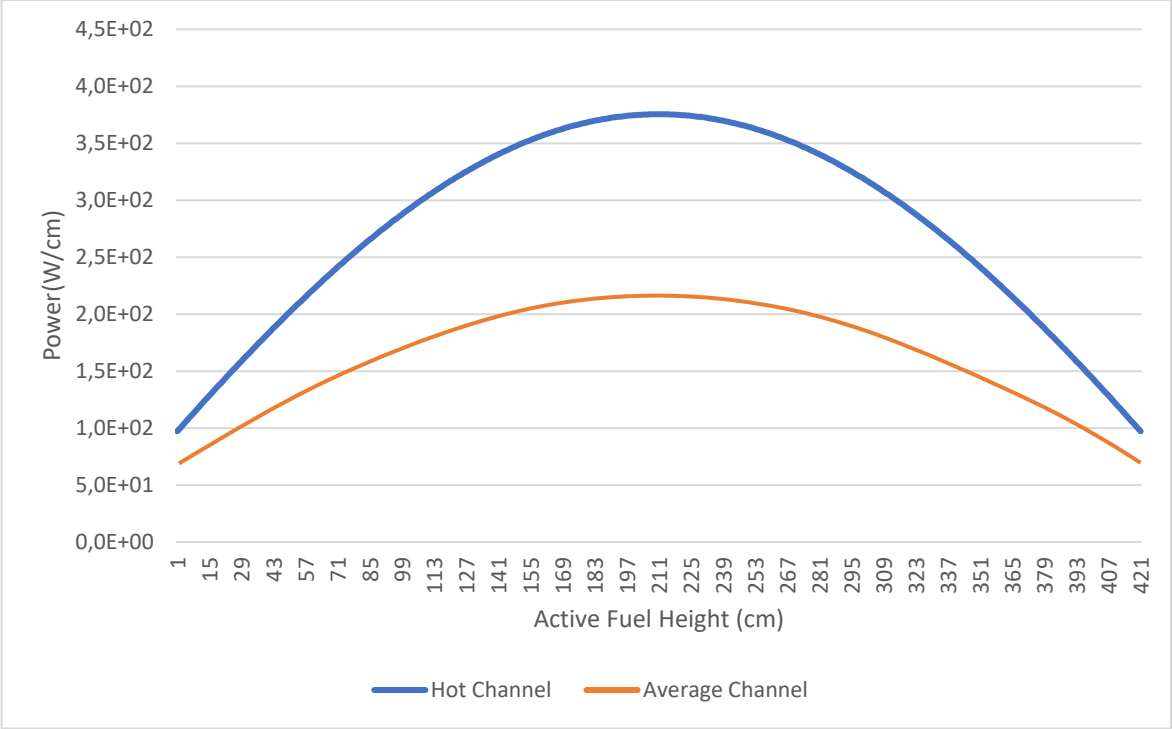

Axial peaking factor (-) 1.35	Radial peaking factor (-) 1.73
Hot channel 354,8 W/cm	Average Channel 204,1W/cm

~~TEMP~~

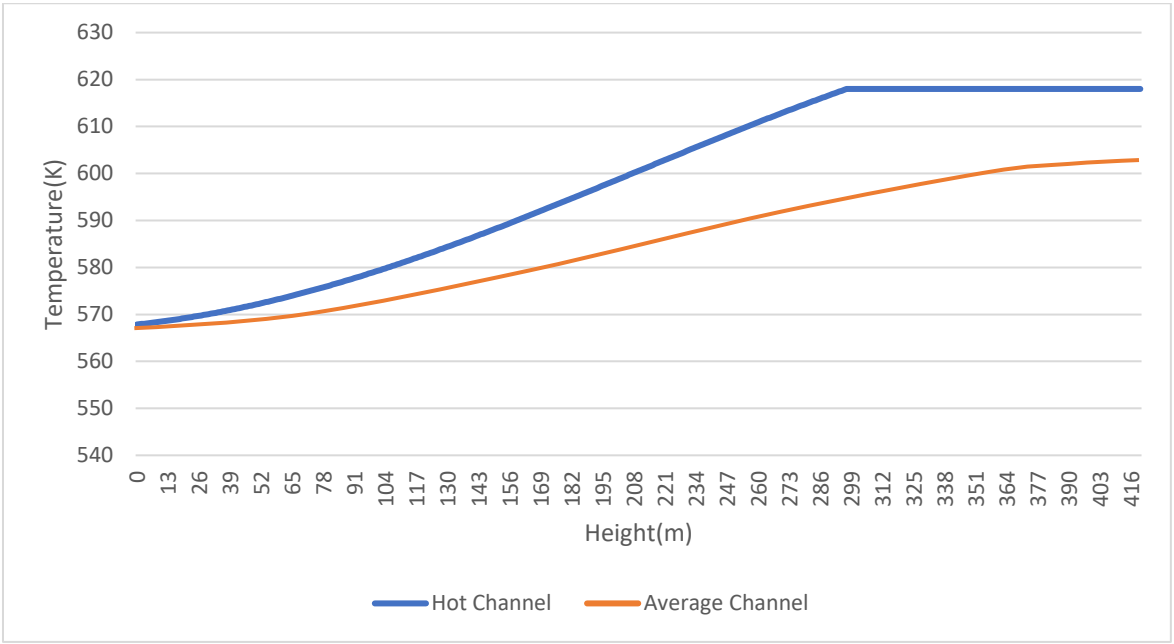

~~ENTHALPY~~

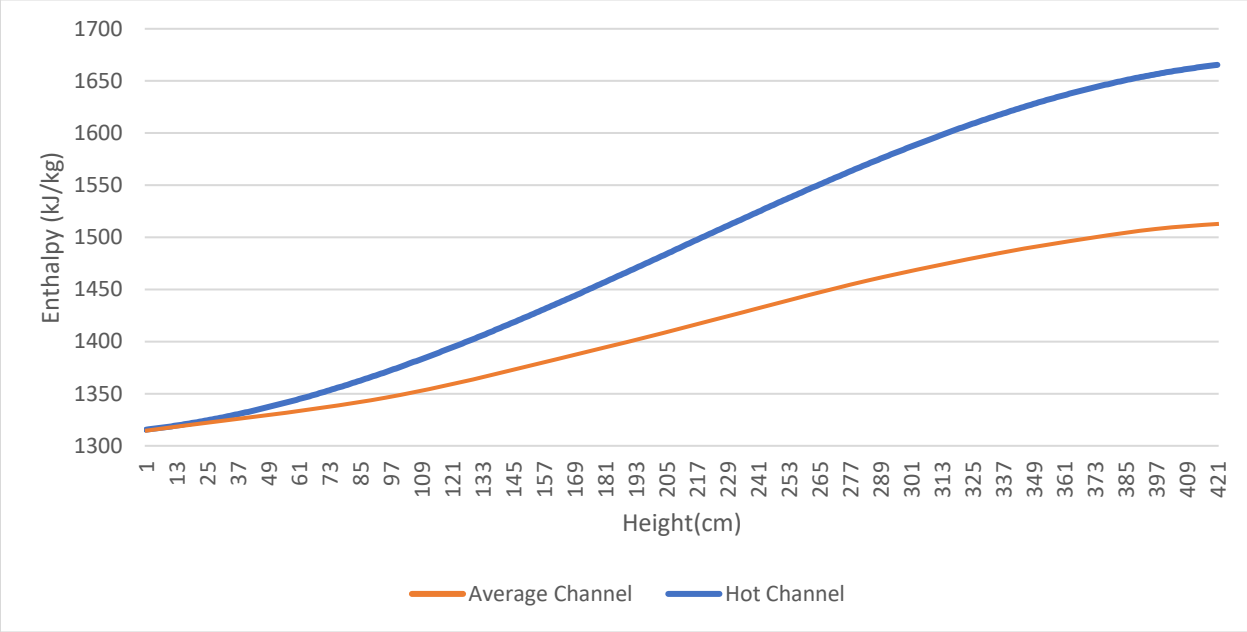

~~PRESSURE~~

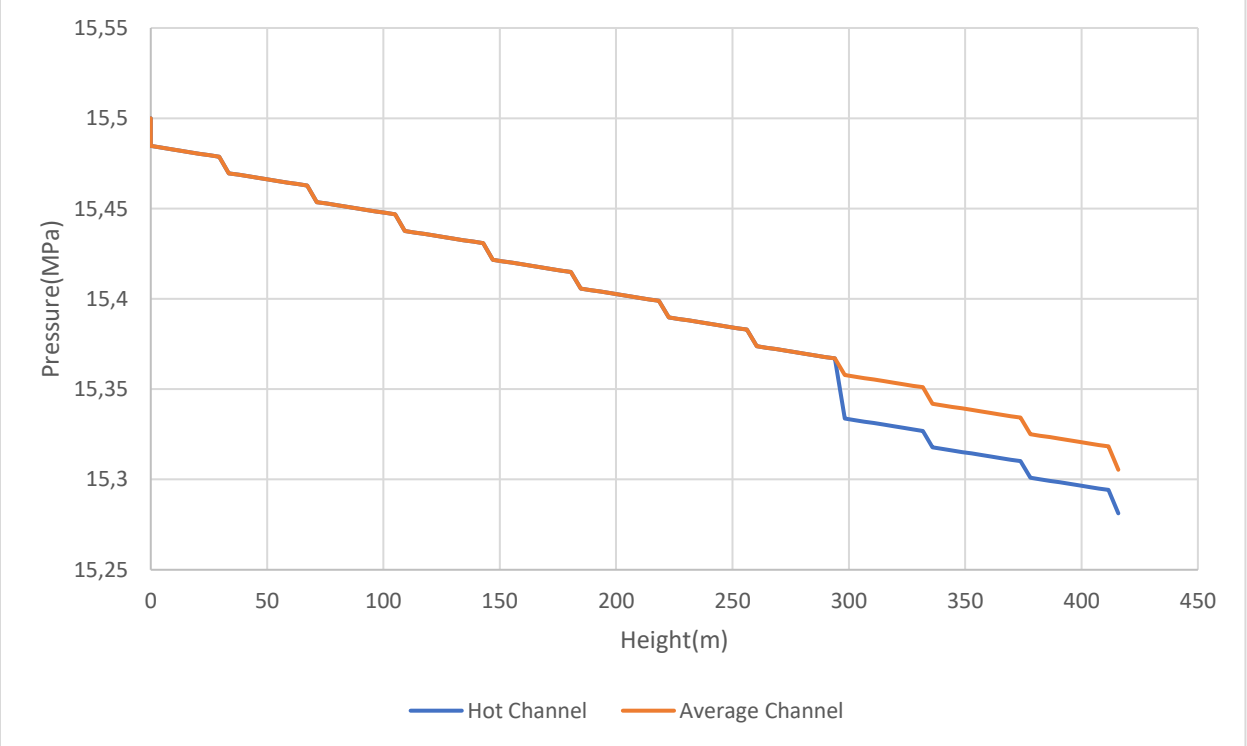

~~DNBR~~

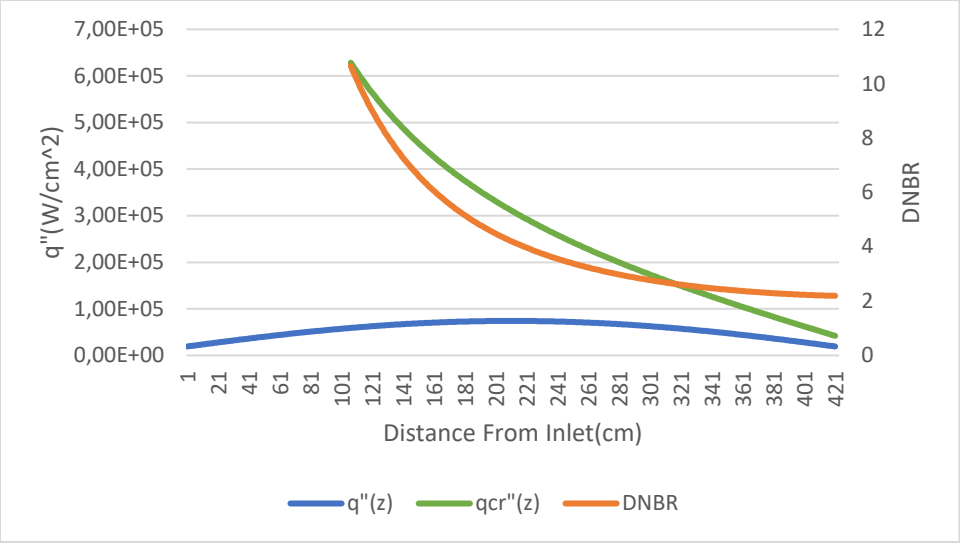

The power density distribution of the hot channel follows the same shape as the average configuration, and the position of maximum power is at the center of the rod. The ratio between the maximum linear power obtained for each configuration is equal to the ratio between the peaking factor applied in each case, which is 1.7383. The temperature distribution plotted using the hot channel follows the same shape as the temperature distribution from the average channel with higher temperature values until z = 296 cm, where the coolant reaches its saturation temperature of 618K °C (saturation temperature for 15.5 MPa). At this point, steam begins to form in the reactor, but the temperature does not continue to increase because the enthalpy is transformed to latent heat instead of sensible heat. The maximum coolant enthalpy value has increased in the hot channel configuration to 1665.39 kJ/kg, and the coolant enthalpy axial distribution has the same shape in both the average and hot channel configurations. In the single-phase flow region where the coolant is fully in the liquid state (z < 298 cm), the pressure drop follows the same evolution in the hot channel configuration as in the average channel configuration. However, when two-phase flow begins, the pressure drops increase, especially in the acceleration pressure drop. Although EPR is not designed to boil, in this calculation, it is observed that the hot channel reaches two-phase towards the top tail of the channel.

Power (MWth)	**Location where Tsat is reached (cm)**
4500	283
4000	231
3600	357
3250	No Boiling

In literature Minimum DNBR under nominal operating conditions nearly 2.6 and in this project MDNBR is 2.2 at 416 cm.

(http://www.epr-reactor.co.uk/ssmod/liblocal/docs/V3/Volume%201%20-%20Overview/1.A%20-%20EPR%20Design%20Description/1.A%20-%20EPR%20Design%20Description%20-%20v3.pdf)

TASK6

CLADDING+FUEL CENTERLINE

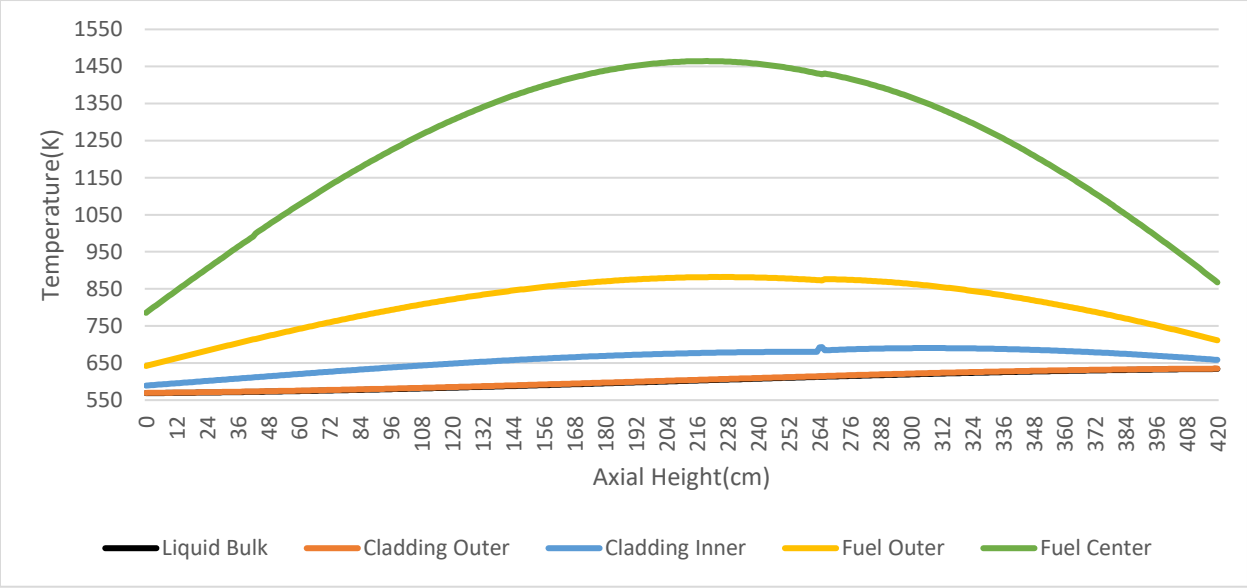

TEMP Diff

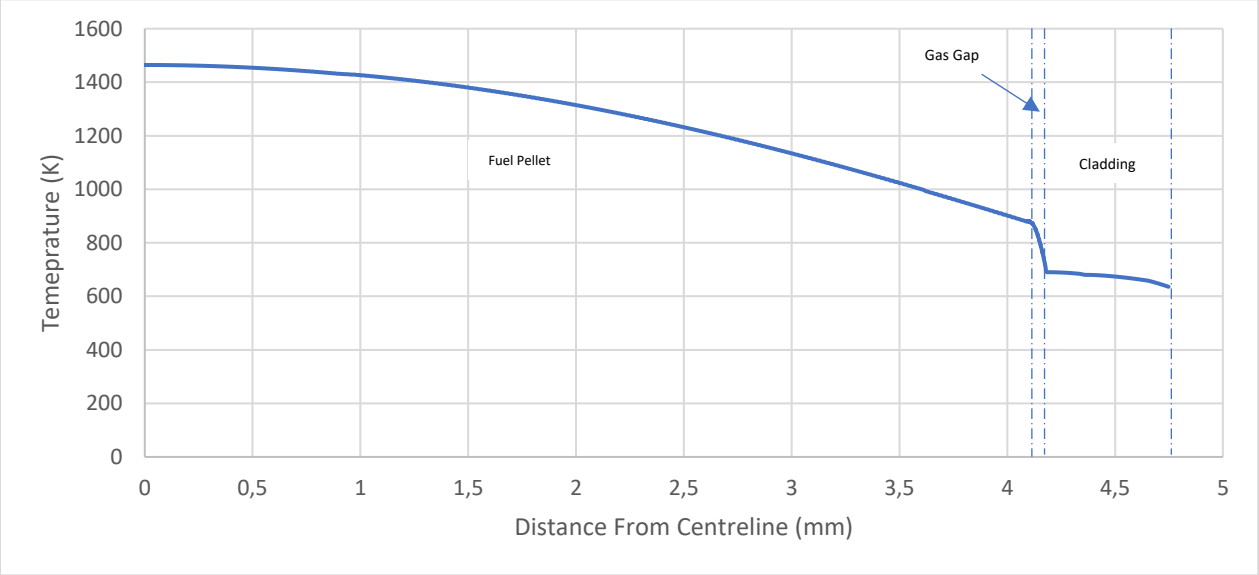

The Figure[ ] shows a slight jump in the cladding inner temperature at 264cm, which is due to the introduction of two-phase flow. At this point, the heat transfer coefficient changes significantly, leading to a notable change in the shape of the temperature curves. Additionally, the cladding surface temperature is very similar to the liquid bulk temperature.

where T is the temperature of the cladding in ◦C, valid between 20-800◦C. For the gas gap, we assumed that it was filled with helium, and used $\lambda G = 3.366 \times 10^{-3} \times T^{0.668}$

using the Reddy Fighetti Subchannel CHF correlation in Eq.(12).

$$q''_{cr}(\mathbf{r}) = B\frac{A - x_{in}}{C + \frac{x(\mathbf{r}) - x_{in}}{q''_R(\mathbf{r})}} \tag{12}$$

where A, B and C are constants and x_{in} is the inlet enthalpy. The applicable range of the correlation is as follows:

$\mathbf{147 < G < 3023}$ kg/m^2 s	$\mathbf{-0.25 < x < 0.75}$	$-1.10 < x_{\text{in}} <= 0.0$
$0.762 < L < 4.267$ m	$6.3 < D_{\text{H}} <= 13.9$ mm	$13.8 < P <= 169.9$ bar

Conditions to apply this correlation are presented above. While this correlation did not fulfil the requirements for the mass flux, there were no correlations provided that met all of the criteria for the EPR so this model was selected as a best estimate.